Short Communication

Maternal mRNA clearance is associated with the prevention of precocious transcription and genome instability in mouse early embryos

Qian-Qian Sha, Yun-Wen Wu, Meng-Yan Jia, Yu Jiang, Xing-Xing Dai, Long-Wen Zhao, Heng-Yu Fan

PII: S2095-9273(25)01053-9

DOI: https://doi.org/10.1016/j.scib.2025.10.030

Reference: SCIB 3644

To appear in: Science Bulletin

Received Date: 17 February 2025 Revised Date: 26 May 2025 Accepted Date: 17 October 2025



Please cite this article as: Q-Q. Sha, Y-W. Wu, M-Y. Jia, Y. Jiang, X-X. Dai, L-W. Zhao, H-Y. Fan, Maternal mRNA clearance is associated with the prevention of precocious transcription and genome instability in mouse early embryos, *Science Bulletin* (2025), doi: https://doi.org/10.1016/j.scib.2025.10.030

This is a PDF file of an article that has undergone enhancements after acceptance, such as the addition of a cover page and metadata, and formatting for readability, but it is not yet the definitive version of record. This version will undergo additional copyediting, typesetting and review before it is published in its final form, but we are providing this version to give early visibility of the article. Please note that, during the production process, errors may be discovered which could affect the content, and all legal disclaimers that apply to the journal pertain.

© 2025 The Authors. Published by Elsevier B.V. and Science China Press All rights are reserved, including those for text and data mining, AI training, and similar technologies.

Maternal mRNA clearance is associated with the prevention of precocious

transcription and genome instability in mouse early embryos

Qian-Qian Sha^{1,2,#}, Yun-Wen Wu^{1,#}, Meng-Yan Jia¹, Yu Jiang¹, Xing-Xing Dai¹, Long-Wen Zhao¹, Heng-Yu Fan^{1,*}

¹ Life Sciences Institute, Zhejiang Key Laboratory of Precise Protection and Promotion of

Fertility, Department of Obstetrics and Gynecology, Sir Run Run Shaw Hospital, School of

Medicine, Zhejiang University, Hangzhou 310058, China

² GMU-GIBH Joint School of Life Sciences, The Guangdong-Hong Kong-Macau Joint

Laboratory for Cell Fate Regulation and Diseases, Guangzhou Medical University, Guangzhou

510006, China

These authors contributed equally to this work.

*Corresponding author.

E-mail address: <u>hyfan@zju.edu.cn</u> (H.-Y. Fan).

Article history:

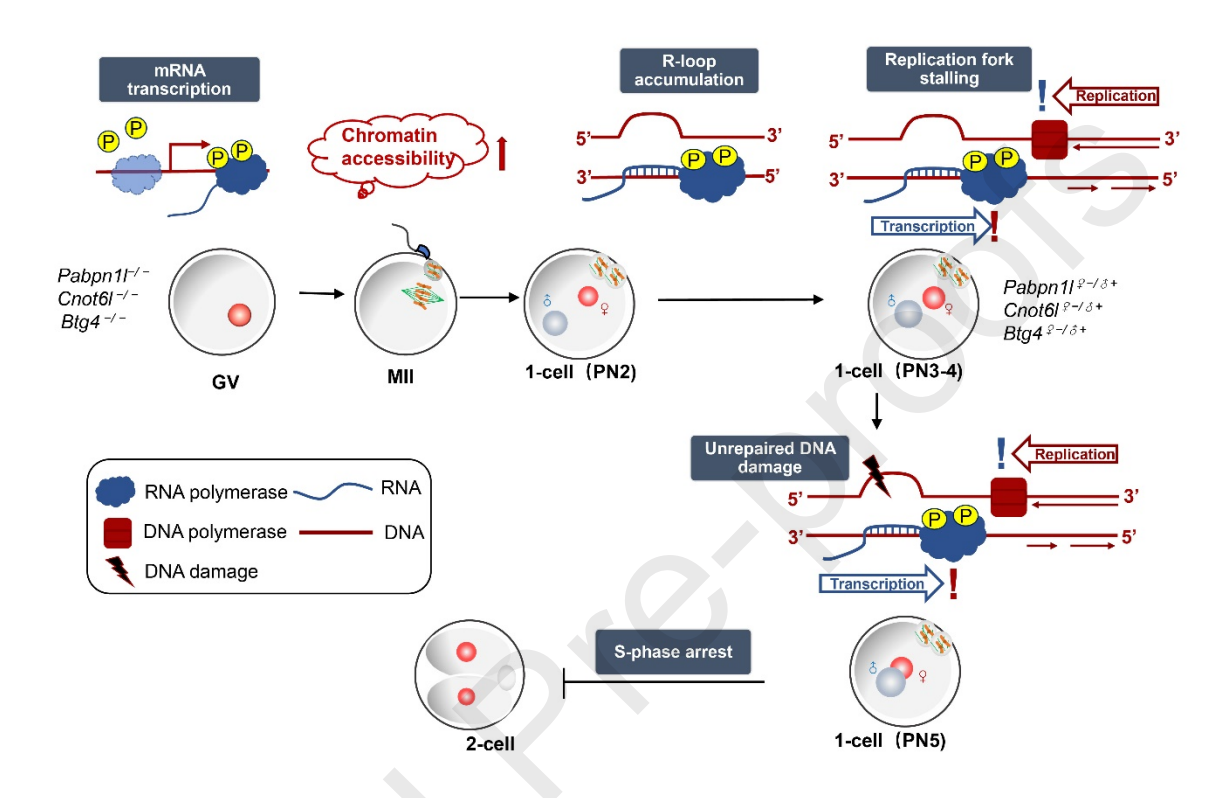
Received 17 February 2025

Received in revised form 26 May 2025

Accepted 17 October 2025

Available online XXX

Graphical abstract



Oocytes accumulate abundant maternal mRNAs during the growth stage of meiotic maturation after transcriptional silencing, and early embryo development prior to zygotic genome activation (ZGA) [1][2]. During the oocyte-to-zygote transition, the selective and stepwise clearance of maternal transcripts is a prerequisite for the initiation of zygotic development [3][4]. Although maternal mutations in mRNA-clearance genes such as poly(A)binding protein nuclear 1-like (*Pabpn11*), CCR4-NOT transcription complex subunit 6-like (*Cnot61*), and BTG anti-proliferation factor 4 (*Btg4*) cause early embryonic arrest, the underlying molecular events remain to be elucidated [5]-[8].

In addition to functioning as templates for protein translation, some maternal mRNAs are physically associated with chromatin, either retained in *cis* at their transcription sites or recruited in *trans* to other genomic regions [9]. To investigate the relationships between mRNA accumulation and chromatin accessibility, we conducted Assay for Transposase Accessible Chromatin with high-throughput sequencing (ATAC-seq) with WT and $Pabpn1l^{Q-/\tilde{O}^+}$ zygotes from PN4-5. Enrichment profiles of ATAC-seq peaks showed that the ablation of Pabpn1l resulted in increased chromatin accessibility, especially at transcription starting sites (TSSs) (Fig. 1a, Fig. S1a online). We found 2074 peaks whose accessibility remained unchanged between $Pabpn1l^{Q-/\tilde{O}^+}$ and WT (Fig. S1b online), 1665 peaks that were only slightly reduced in $Pabpn1l^{Q-/\tilde{O}^+}$ (Fig. S1c online), and most strikingly 2154 peaks that became aberrantly open

in $Pabpn1l^{Q-/O+}$ (Fig. S1d online). The fold changes of these aberrantly opened peaks were substantially larger than the reductions observed in the other two clusters (Fig. S1b-d online). We identified 2659 genes with accessible promoters in WT zygotes and 1105 exclusively in $Pabpn1l^{Q-/O+}$ zygotes (Fig. 1b). Genes whose promoters became exclusively accessible in $Pabpn1l^{Q-1/\tilde{O}+}$ exhibited a pronounced increase in accessibility. While genes with shared accessibility between WT and $Pabpn1l^{Q-1/Q+}$ also showed a modest increase, the magnitude was far smaller than that observed for $Pabpn11^{q-1/3}$ -exclusive genes (Fig. S1e online). To specify their expression dynamics, we analyzed published single-cell RNA sequencing (scRNA-seq) data from zygotes at different post-fertilization time points [10]. Heatmap profiling of the genes whose promoters are accessible in wild-type embryos showed a progressive rise in transcript abundance from 6–10 h post-fertilization, with the majority exhibiting sustained up-regulation (Fig. 1c, left). However, among the $Pabpn11^{Q-1/\tilde{C}^+}$ -exclusive genes, only 46.73% exhibited a sustained upward trend between 6 and 10 h (Fig. 1c, right), which is markedly lower than the 62.83% observed in the wild-type. Particularly, WT-only accessible chromatin regions harbour over 20% more ZGA-associated genes than those unique to the $Pabpn11^{Q-1/\tilde{G}^+}$ (Fig. 1d), highlighting the pronounced enrichment of ZGA genes in the WT context. In contrast, the $Pabpn1l^{Q-1/\tilde{O}^+}$ exclusive genes appear to be enriched for maternally derived transcripts, suggesting that the mutant retains a larger maternal gene expression program. Snapshots further demonstrated that the promoter regions of ZGA genes (e.g., Pan2, Dux) exhibited reduced accessibility, whereas maternal genes (e.g., Zp3, Gdf9) displayed pronounced accessibility in $Pabpn1l^{Q-/Q+}$ zygotes compared to WT (Fig. 1e). To assess whether increased chromatin accessibility at TSSs in $Pabpn11^{Q-/\tilde{C}+}$ zygotes increases transcriptional activity, we performed immunofluorescent (IF) analysis with 5-ethynyluridine (EU). As expected, EU signals were detected in transcriptionally active growing oocytes with a non-surrounded nucleolus (NSN) configuration, while absent in transcriptionally silenced fully grown oocytes with a surrounded nucleolus (SN), confirming the assay's sensitivity and specificity (Fig. S2a online). WT zygotes exhibited detectable transcription only at the PN4 stage as previously reported [11], while $Pabpn1l^{Q-/Q+}$ zygotes showed aberrant transcriptional activation with detectable EU incorporation as early as PN2 (Fig. 1f, g). This activity intensified at PN3 and remained elevated compared to WT at PN4-5 stages (Fig. 1f, g, Fig. S2b, c online). Similarly, $Btg4^{\circ -/\circ +}$ zygotes also displayed increased transcriptional activity at the PN5 stage (Fig. S2d, e online).

Traditional RNA sequencing cannot determine if excessive transcription is from ZGA or maternal mRNAs due to maternal transcripts in the ooplasm. As shown in Fig. 1h, oocytes and embryos were cultured in 4-Thiouridine (S⁴U) medium for 2 h, followed by alkylation to induce U-C mismatches in nascent RNAs during reverse transcription. Nascent RNAs were identified by aligning reads to the reference genome (Table S2 online). To verify this method, S4U-seq was performed on MII oocytes, zygotes, and two-cell embryos from 4-week-old WT mice. Consistently, transcriptionally silent MII oocytes showed minimal global U-C mutation ratios (Fig. S3a-c online). However, the global U-C mutation ratios in oocytes/embryos were much lower than those in 293T cells (Fig. S3a-e online). We speculate that massive RNA storage in oocytes may contribute to the relatively low ratio of global U-C mutations. In the two-cell embryos, 1832 nascent RNA signals, including typical ZGA genes such as Zscan12, Zscan4d, and Dux, were identified (Fig. S3f online). Meanwhile, zygotes exhibited progressive nascent RNA accumulation consistent with established ZGA timelines [10] (84.41% of transcripts upregulated 6-10 h post-fertilization) (Fig. 1i). A Venn diagram showed that nascent RNA identified in zygote and two-cell embryos had 52.3% overlapping signals, reflecting the continuous occurrence of ZGA (Fig. 1j). $Pabpn1l^{Q-/\tilde{C}+}$ zygote had a higher mutation ratio than

that in WT zygote (Fig. S3b and d online). Notably, S⁴U-seq revealed significant transcriptional dysregulation in $Pabpn11^{Q-1/Q+}$ zygotes, which displayed both elevated global U-C conversions (1359 vs. 924 in WT) (Fig. 1k) and a near two-fold increase in mutant-specific nascent RNA signals (Fig. 11). About half of the nascent genes were also accessible according to the ATACseq (Fig. S3g online). Although the majority of the accessible genes did not generate nascent RNA, it has been known that nascent RNA expression exhibits a slight delay relative to chromatin accessibility captured by ATAC-seq [12]. However, the overlap of nascent RNAs identified in WT two-cell and $Pabpn1l^{\varphi-/\circlearrowleft+}$ zygotes showed that the aberrant transcription of $Pabpn1l^{Q-/\tilde{G}+}$ zygotes was not caused by the elevated expression of major ZGA genes (Fig. 1m, Fig. S3h online). Comparative analysis demonstrated that precocious transcription primarily originated from failed maternal transcript clearance (Fig. 1n). 45.5% of nascent-RNAs originated from genes whose transcript levels increased at least two-fold due to defects in maternal mRNA degradation [6] (Fig. 1n). Consistently, 56.8% of the nascent RNAs in mutant zygotes were derived from the same genes that gave rise to maternal mRNAs (Fig. 1o), and most nascent RNAs up-regulated by more than 2-fold in mutant zygotes also originate from genes that produce maternal transcripts (Fig. 1p). We validated this trend individually for several maternal genes; all exhibited a markedly increased mutation rates in $Pabpn1l^{2-/3+}$ zygotes (Fig. S3i online). Notably, maternal genes such as *Kifc3* exhibit higher transcript levels in WT, while aberrant transcription of previously silenced maternal genes emerges in $Pabpn1l^{Q-1/\tilde{C}}$ zygotes. The dysregulation indicates a genome-wide failure to suppress maternal programs in $Pabpn1l^{Q-/O^+}$ zygotes. Corroborated by parallel ATAC-seq data revealing increased chromatin accessibility, the findings indicated aberrant transcription in $Pabpn1l^{Q-/\circlearrowleft+}$ zygotes was driven by both indirect (chromatin remodeling) and direct (template availability) mechanisms.

R-loop is formed when nascent RNA re-anneals to the DNA template strand [13]. Using the S9.6 antibody, we detected excessive R-loop accumulations in $Cnot6l^{Q-/\tilde{G}+}$ and Pabpn11 $^{Q-/Q+}$ zygotes at PN4-5. Treatment with α -amanitin, a transcription inhibitor, eliminated S9.6 signals in both WT and $Pabpn11^{\varphi-/\tilde{O}+}$ zygotes (Fig. 2a, b), indicating that Rloop formation requires active transcription. Overexpression of RNase H1 (an RNA: DNAhybrid-specific endonuclease) reduced S9.6 signals, whereas a catalytically inactive mutant (RNase H1WKKD) had no effect (Fig. 2c, d). We next examined whether R-loop accumulation correlates with DNA damage and developmental defects. In WT zygotes, transient pH2AX (pH2AX-S139) signals (marking DNA damage) appeared at PN3-4 but resolved by PN5 (Fig. S4a, b online). In contrast, the $Pabpn1l^{\varphi-/\mathring{\circlearrowleft}^+}$, $Cnot6l^{\varphi-/\mathring{\circlearrowleft}^+}$, and $Btg4^{\varphi-/\mathring{\circlearrowleft}^+}$ zygotes exhibited persistently elevated pH2AX at PN3-5 (Fig. 2e, f and Fig. S4a-d online). A subset of $Cnot6l^{\varphi-/\Diamond+}$ zygotes progressed to the two-cell stage but arrested with abundant nuclear γ H2AX (Fig. S4e, f online). Additionally, RPA2, a marker of single-strand DNA breaks, was also elevated in all mutant zygotes (Fig. S4g, h online). To test whether R-loops directly contribute to DNA damage, we overexpressed Rnasehl in Pabpull $^{\mathbb{Q}-/\mathcal{O}+}$ zygotes. RNase H1, but not RNase H1WKKD, reduced pH2AX to undetectable levels, even below the WT baseline (Fig. 2e, f), suggesting that excessive R-loops drive DNA damage in maternal RNA decay mutants.

We further assessed the possible role of maternal factors in regulating the first round of DNA replication in zygotes, as indicated by the 5-ethynyl-2'-deoxyuridine (EdU) incorporation

assay. To confirm the specificity of EdU incorporation, aphidicolin, a DNA polymerase inhibitor, eliminated EdU signals in cultured WT zygotes (Fig. S5a online). This treatment also induced DNA double-strand breaks (DSBs) and RPA2 foci formation, mimicking the genomic instability seen in maternal Pabpn1l/Cnot6l-deleted zygotes (Fig. S5a-c online). DNA replication in WT zygotes was initiated at the PN3 stage and finished at the early PN5 stage (Figs. S5a and S6a-c online). In contrast, in $Pabpn11^{\varphi-/\tilde{G}+}$ zygotes, DNA replication also initiated at PN3 but progressed more slowly, remaining incomplete at late PN5. Significantly decreased EdU incorporation at the PN4 stage and prolonged DNA replication at the PN5 stage were also observed in $Pabpn1l^{\varphi-/\Diamond}$ and $Cnot6l^{\varphi-/\Diamond+}$ zygotes (Fig. S6b–d online). Even as control zygotes reached the two-cell stage and began the second round of replication, EdU signals persisted in arrested $Cnot6l^{Q-/\tilde{S}+}$ zygotes, or were weakly detected in those two-cell stage $Cnot6l^{\varphi-/\Diamond}$ embryos (Fig. S6e, f online). These mutant zygotes also showed persistent FANCD2 (S-phase checkpoint marker) and diminished pH3S10 (a G2/M phase marker) signals (Fig. S6g-j online), indicating S-phase arrest. More importantly, DNA replication defects in $Pabpn1l^{2-/3+}$ zygotes were also rescued by RNase H1 overexpression, as reflected by increased EdU incorporation at the PN4 stage and termination of EdU incorporation at the PN5 stage (Fig. 2g, h). RNaseH1 overexpression also improved developmental progression (Fig. 2i) and elevated ZGA gene expression (Fig. 2j), demonstrating R-loop-mediated replication stress as the primary defect.

Our data suggest that defective maternal mRNA clearance is associated with precocious transcription and changes in chromatin accessibility in both oocytes [14] and zygotes. Undegraded maternal transcripts (e.g., histone-modifying enzymes, chromatin remodelers) could maintain an 'oocyte-like' chromatin state incompatible with zygotic genome activation. Another possibility is that maternal genes have distinct regulatory elements or chromatin structures that make them more susceptible to the effects of impaired maternal mRNA clearance. Ectopic transcription forms pathological R-loops that obstruct replication forks. The resulting collisions trigger genomic instability, activate the S-phase checkpoint, and ultimately arrest embryonic development (Fig. S7 online). Our findings mechanistically link maternal mRNA clearance to three essential zygotic processes: (1) chromatin reprogramming, (2) transcription regulation, and (3) replication fidelity. Definitive mechanistic proof will require future experiments—such as oocyte-specific rescue or acute degradation of maternal transcripts—that are technically beyond the scope of the present study.

Conflict of interest

The authors declare that they have no conflict of interest.

Acknowledgments

This work was supported by the National Natural Science Foundation of China (31930031 and 32270894), the National Key Research and Development Program of China (2024YFA1803000 and 2021YFA1100300), the Natural Science Foundation of Zhejiang Province (LD22C060001), the Guangdong Basic and Applied Basic Research Foundation

(2022B1515020038), and the Guangzhou Science and Technology Project (202201011005).

Author contributions

Heng-Yu Fan and Qian-Qian Sha conceived, designed, and supervised the study. Heng-Yu Fan and Qian-Qian Sha wrote the manuscript. Qian-Qian Sha, Yun-Wen Wu, Meng-Yan Jia, Yu Jiang, Xing-Xing Dai, and Long-Wen Zhao performed the mouse experiments. Yun-Wen Wu performed the high-throughput sequencing experiments and analyzed the data.

Data availability

S⁴U-seq data were deposited in the NCBI Gene Expression Omnibus database under the accession code GSE279466.

ATAC-seq data were deposited in the NCBI Gene Expression Omnibus database under the accession code GSE279465.

Appendix A. Supplementary material

Supplementary data to this article can be found online.

References

- [1] Conti M, Franciosi F. Acquisition of oocyte competence to develop as an embryo: integrated nuclear and cytoplasmic events. *Hum Reprod Update* 2018;24:245-266.
- [2] Sha QQ, Zhang J, Fan HY. A story of birth and death: mRNA translation and clearance at the onset of maternal-to-zygotic transition in mammals. *Biol Reprod* 2019;101:579-590.
- [3] Sha QQ, Zhu YZ, Li S, et al. Characterization of zygotic genome activation-dependent maternal mRNA clearance in mouse. *Nucleic Acids Res* 2020;48:879-894.
- [4] Sha QQ, Zheng W, Wu Y-W, et al. Dynamics and clinical relevance of maternal mRNA clearance during the oocyte-to-embryo transition in humans. *Nat Commun* 2020;11:4917.
- [5] Yu C, Ji SY, Sha QQ, et al. BTG4 is a meiotic cell cycle-coupled maternal-zygotic-transition licensing factor in oocytes. *Nat Struct Mol Biol* 2016;23:387-394.
- [6] Zhao LW, Zhu YZ, Chen H, et al. PABPN1L mediates cytoplasmic mRNA decay as a placeholder during the maternal-to-zygotic transition. *EMBO Rep* 2020;21:e49956.
- [7] Sha QQ, Yu JL, Guo JX, et al. CNOT 6L couples the selective degradation of maternal

- transcripts to meiotic cell cycle progression in mouse oocyte. EMBO J 2018;37:e99333.
- [8] Zheng W, Zhou Z, Sha Q, et al. Homozygous mutations in BTG4 cause zygotic cleavage failure and female infertility. *Am J Hum Genet* 2020;107:24-33.
- [9] Li X, Fu XD. Chromatin-associated RNAs as facilitators of functional genomic interactions. *Nat Rev Genet* 2019;20:503-519.
- [10] Asami M, Lam BYH, Hoffmann M, et al. A program of successive gene expression in mouse one-cell embryos. *Cell Rep* 2023;42:112023.
- [11] Sakashita A, Kitano T, Ishizu H, et al. Transcription of MERVL retrotransposons is required for preimplantation embryo development. *Nat Genet* 2023;55:484-495.
- [12] Li M, Jiang Z, Xu X, et al. Chromatin accessibility landscape of mouse early embryos revealed by single-cell NanoATAC-seq2. *Science* 2025; 387:eadp4319.
- [13] García-Muse T, Aguilera A. R Loops: from physiological to pathological roles. *Cell* 2019;179:604-618.
- [14] Chousal J, Cho K, Ramaiah M, et al. Chromatin modification and global transcriptional silencing in the oocyte mediated by the mRNA decay activator ZFP36L2. *Dev Cell* 2018;44:392-402.

Figure legends

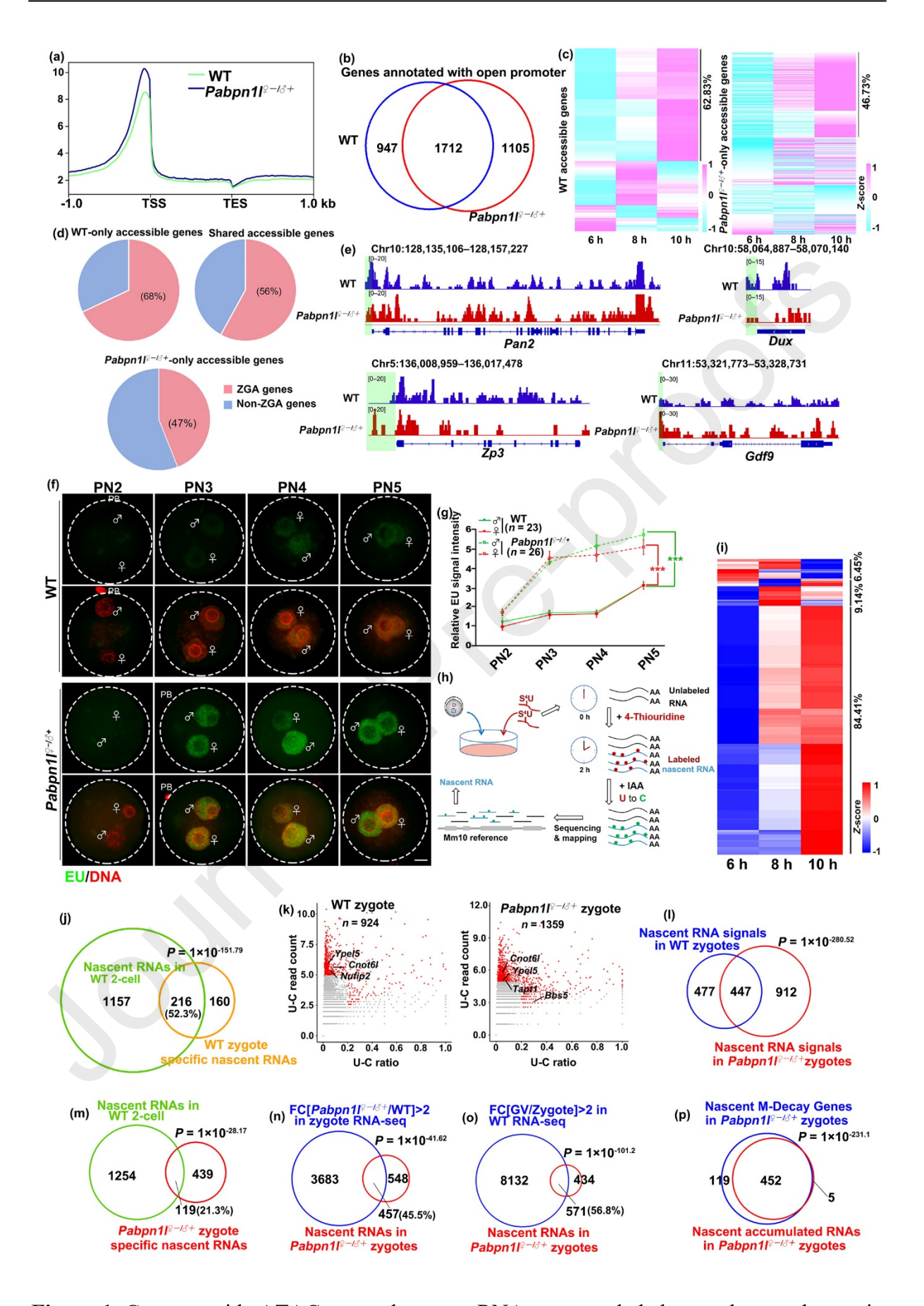


Figure 1. Genome-wide ATAC-seq and nascent RNA seq revealed abnormal open chromatin

areas and synthesized transcription of $Pabpn1l^{Q-1/Q+}$ zygotes. (a) Enrichment profiles showing the fluctuation of ATAC signals in zygotes collected from WT or $Pabpn1l^{\frac{n}{2}-\frac{n}{2}}$ mice. (b) Venn diagram showing the number of genes annotated with open chromatin signals in their promoters in WT and $Pabpn11^{Q-/Q+}$ zygote groups, respectively, and overlaps. (c) Heatmap indicating expression level (FPKM) of transcripts with open promoter identified in WT and $Pabpn1l^{\varphi-/\Diamond+}$ only accessible genes. Expression level data were extracted from published scRNA-seq with Zscore calibration. 6, 8, and 10 h refer to 6, 8, and 10 hours after fertilization. Percentages in the right panel indicated the proportion of genes from three different expression pattern groups. (d) Pie chart showing the ZGA ratio of WT-specific, shared, and Pabpn112-13+-specific open promoter genes. (e) Snapshots showing open chromatin areas represented by ATAC-seq peaks. Promoter regions were indicated by a green shade. (f) EU (5-ethynyl uridine) incorporation signals in WT and $Pabpn11^{Q-1/Q+}$ zygotes. Scale bar represents 10 µmol/L. (g) Quantification of the EU signals in (f). Error bars, s.e.m. ***P < 0.001 by two-tailed Student's t-test. (h) Flow diagram showing the process of S⁴U-seq. (i) Heatmap indicating expression level (FPKM) of transcripts with nascent RNA signals identified in WT zygote S⁴U-seq. Expression level data were extracted from published scRNA-seq with Z-score calibration. 6 h, 8 h, and 10 h refer to 6, 8, and 10 hours after fertilization. Percentages in the right panel indicated the proportion of genes from three different expression pattern groups. (j) Venn diagram indicating the overlap of nascent transcripts with positive signals detected in WT two-cell and WT-zygote-specific nascent RNA. (k) Scatter diagram showing positive nascent RNA signals detected in S⁴U-seq. Criterion used in the case, including T-C ratio > 0.2 and total reads > 20; T-C ratio < 0.2 and total reads > 30. (1) Venn diagram showing the number of positive signals in WT and $Pabpn1l^{2-1/3+}$ S⁴U-seq and overlaps. (m) Venn diagram indicating the overlap of nascent transcripts with positive signals detected in WT two-cell and $Pabpn1l^{Q-/\tilde{G}+}$ zygote-specific nascent RNA. (n) Venn diagram indicating the overlap of genes whose transcript levels in PabpnIl^{2-/♂+} zygotes were more than twice those in WT and nascent RNA detected in S⁴Useq at the $Pabpn1l^{Q-/\partial^+}$ zygote stage. (o) Venn diagram indicating the overlap of maternal decay genes (decreased two-fold from WT GV to zygote stage in RNA-seq) and nascent RNA detected in S⁴U-seq at $Pabpn1l^{Q-/O+}$ zygote stage. (p)Venn diagram indicating overlap between the overlapped 457 genes in Fig. 1n and the overlapped 571 genes in Fig. 1o.

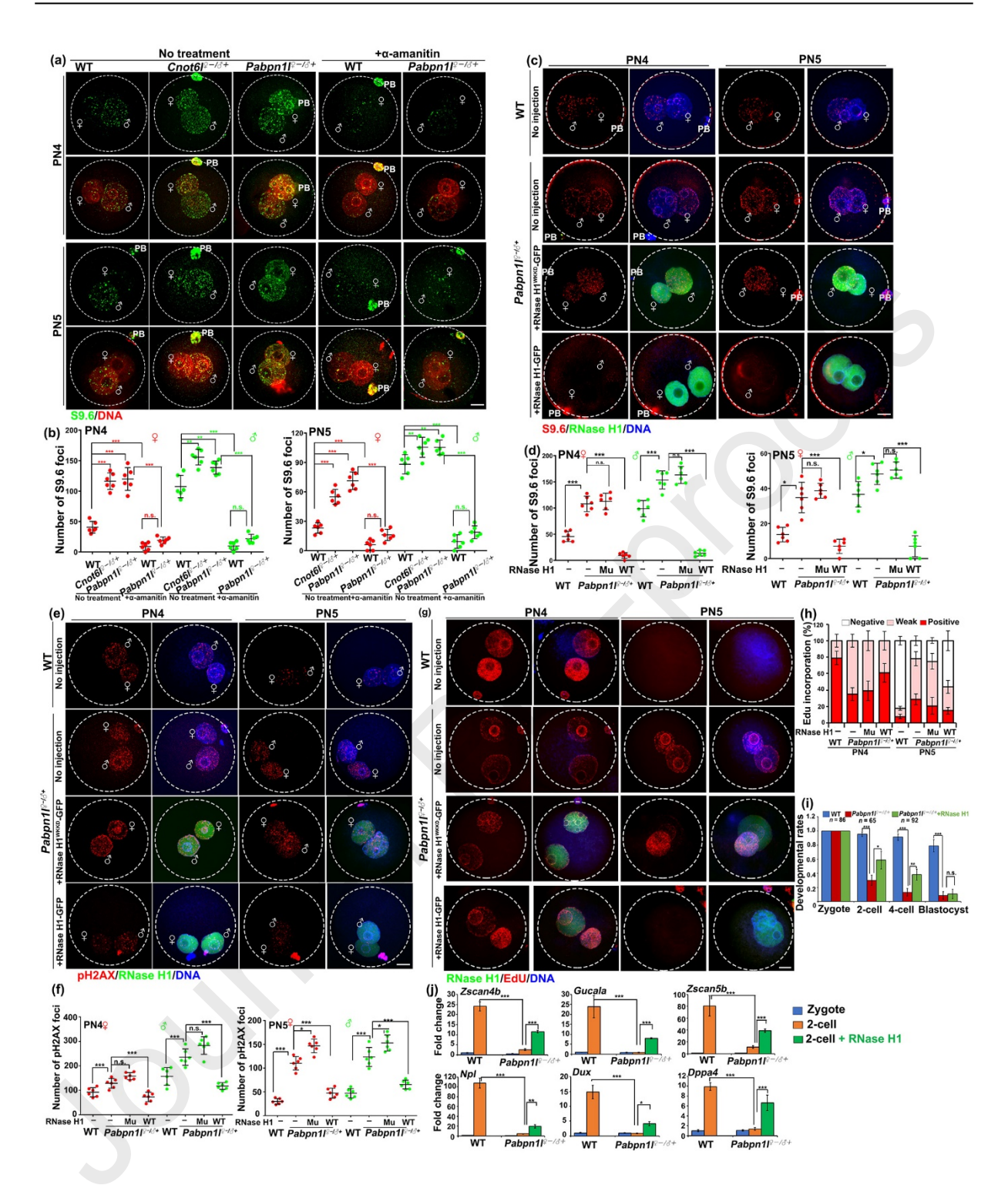


Figure 2. Impacts of ectopic RNase H1 expression on R-loop formation, DNA damage, and DNA replication in $Pabpn1l^{Q-/Q^+}$ zygotes. (a) Immunofluorescence results showing the RNase H1 and S9.6 monoclonal antibody signals in zygotes of the indicated genotypes. To inhibit transcription, some zygotes were collected from oviducts at 22 h after hCG injection and incubated with α-amanitin (5 ng/μL) for 2 h before immunostaining. Scale bars represent 10 μmol/L. (b) Quantifications of S9.6 foci in (a). Error bars, s.e.m. **P < 0.01 and ***P < 0.001 by two-tailed Student's *t*-test. n.s.: non-significant. (c) Detection of GFP-RNase H1 (WT and catalytic site mutated form) expression and S9.6 monoclonal antibody-labeled signals in

zygotes of the indicated genotypes. Scale bars represent 10 µmol/L. (d) Quantifications of S9.6 foci in (c). Error bars, s.e.m. *P < 0.05 by two-tailed Student's t-test. (e) Detection of pH2AX signals in WT and $Pabpn1l^{Q-/\tilde{G}^+}$ zygotes microinjected with mRNAs encoding GFP-RNase H1 (WT and catalytic site mutated form). Scale bars represent 10 µmol/L. (f) Quantifications of pH2AX foci in (e). Error bars, s.e.m. (g) Detection of GFP-RNase H1 expression and EdU incorporation signals in zygotes of the indicated genotypes. Scale bar represents 10 µmol/L. (h) Quantifications of EdU incorporation signals in (g). Error bars, s.e.m. (i) Proportions of WT and $Pabpn1l^{Q-/\tilde{G}^+}$ zygotes developing to the indicated stages, with or without ectopic RNase H1 expression. (j) qRT-PCR results show the mRNA expression levels of representative early zygotic genes. In (i–j), Error bars, s.e.m. *P < 0.05, **P < 0.01, and ***P < 0.001 by two-tailed Student's t-test.